Available online at www.sciencedirect.com
SCIENCE DIRECT®
Journal of Power Sources 122 (2003) 201–209
JOURNAL OF POWER SOURCES
www.elsevier.com/locate/jpowsour

Mathematical simulation of thermoelectric power generation with the multi-panels

Ryosuke O. Suzuki*, Daisuke Tanaka

Department of Energy Science and Technology, Kyoto University, Yoshida-Honmachi, Sakyo-Ku, Kyoto 606-8501, Japan

Received 1 October 2002; received in revised form 6 February 2003; accepted 17 February 2003

Abstract

Electric power was estimated in case of the large-scale flat thermoelectric panels exposed to two thermal fluids. The output powers of the proposed 15 systems were analytically deduced from heat transfer theory, and written by non-dimensional functions to reflect the characteristics of system design. The maximum output was the largest in the ideal isothermal systems. In the other realistic systems, it was the largest for the system of the counter flow with one panel. The multiplication of thermoelectric panels can shorten significantly the device area, although the output from the multi-panels decreases a few percent. The worse heat conductivity, λ of thermoelectric materials and the better heat transfer at the surfaces are desired for these fluid systems, in addition to the better figure of merit, Z.

Keywords: Thermoelectric generation; Thermoelectric device; Heat transfer; Thermal fluid; Figure of merit

1. Introduction

Seebeck effect on the junctions of two different materials can generate the thermoelectric power, P depending on a temperature difference. Because we can not use the infinitively large heat bath practically, this ideal case should be modified. It is designed that a thermal energy is extracted by a fluid and passed to the thermoelectric generator. There, hot and cold fluids offer the temperature difference between the two surfaces of the plane thermoelectric modules. The thermoelectric motive force, E in the open circuit is the sum of multiplication of the relative Seebeck coefficient, α and the temperature difference, ΔT over all the serial connections. The problem to obtain the larger P is, therefore, how we give the lager ΔT for all the thermo-elements, because α is determined only by the materials used for the thermoelectric panel.

The heat applied at the hot junction is scattered and lost at the cold junction, corresponding to the temperature gradient inside the thermoelectric panel. The heat from the hot fluid is passed to the panel surface by heat transfer, to the cold surface by heat conduction through the solid, and finally to the cold fluid again by heat transfer. The fluids are resultantly warmed or cooled along the flow path, and their temperature profile through the path, $T(x)$, changes as a function of position, x. This kind of problem is known as the problem at heat exchanger through an isolator [1]. Additionally as the special feature in the thermoelectric power generation, the heat transfer due to Peltier effect and Joule heating should be considered [2,3].

The purpose of this work is to show the mathematical expression of the maximum power extractible from the thermoelectric panel which is heated by the hot fluid and cooled by the cold fluid. The heat transfer through the panel and the temperature change along the fluid path are analyzed mathematically. Mathiprakasam et al. reported the precise analysis using Laplace transformation [3]. Their solution was very complex form due to Peltier effect and Joule heating although a sheet of panel was studied.

It was expected that a compact system for the large-scale power generation could be realized by the multi-sheets of panel, which were efficiently given the larger ΔT by the multi-fluid paths [4,5]. As we proposed previously the concept to use this kind of multi-layered panels [4], the heat loss through a thermoelectric panel is recovered by another fluid, and the captured heat is passed to another thermoelectric panel. We hope that the efficient recovery of thermal energy in a restricted space may become possible by solving the necessary thermal and fluid conditions. Esarte et al. considered the temperature drop during circulation of fluid, and showed that it was fairly large [5].

Here we propose 15 kinds of thermoelectric power generation system with multi-panels. Applying the heat

* Corresponding author. Tel.: +81-75-753-5453; fax: +81-75-753-5432.
E-mail address: suzuki@energy.kyoto-u.ac.jp (R.O. Suzuki).

0378-7753/03/$ – see front matter © 2003 Elsevier Science B.V. All rights reserved.
doi:10.1016/S0378-7753(03)00396-3

transfer analysis, we solve analytically their temperature profiles $T(x)$ and output power, P using the matrix analysis. Non-dimensional descriptions enable us to select the best system, independently of the thermophysical properties of the thermoelectric materials and working fluids.

2. Basic assumptions and models

2.1. Flat plane panels

It is assumed that all of our thermoelectric panels are flat, and that they consist of the thermoelements with a single layer of Π-type pn junctions, as illustrated in Fig. 1. The thermoelements are homogeneously aligned perpendicular to heat flow, combined tightly without open space, and connected electrically in series. The hot and cold fluids flow along the both flat surfaces of the panel, and they are isolated by the panel. Practically, as shown in Fig. 1, there exist the electrodes connecting the thermoelements, the open space between them, the protective film between the fluid and the thermoelements, and the fins that enhance the heat exchange. Esarte et al. proposed to circulate the fluid in a path to enhance heat transfer [5]. Here for simplicity we neglected these effects on heat transfer, or considered them as the heat transfer coefficient at the surfaces.

This work will discuss the shape and system holding multi-planes. The number of the planes, n the directions of hot and cold fluids, and the path shape for fluids are classified systematically as below.

2.2. Directions of fluids

Firstly the fluid directions are classified into four types, depending on the direction of cold fluid at the exist of the corresponding hot fluid: parallel flow type (P), counter flow type (C), isothermsal type (I) and the mixed type (X), as shown in Fig. 2. We assume only one path for each fluid. Namely, we set the boundary conditions that each system has only two paths connecting in series.

The parallel flow type is the system that the two fluids flow in the same direction, between which the thermoelectric panel is inserted. The fluids flow in the opposite direction

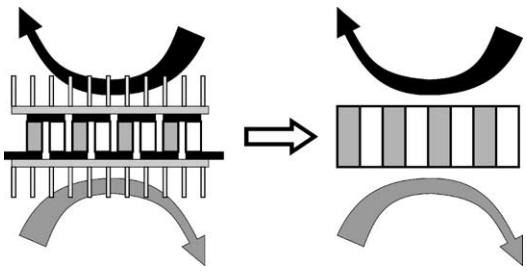

Fig. 1. Simplification of thermoelectric module. Two fluids flow over the smooth flat panel.

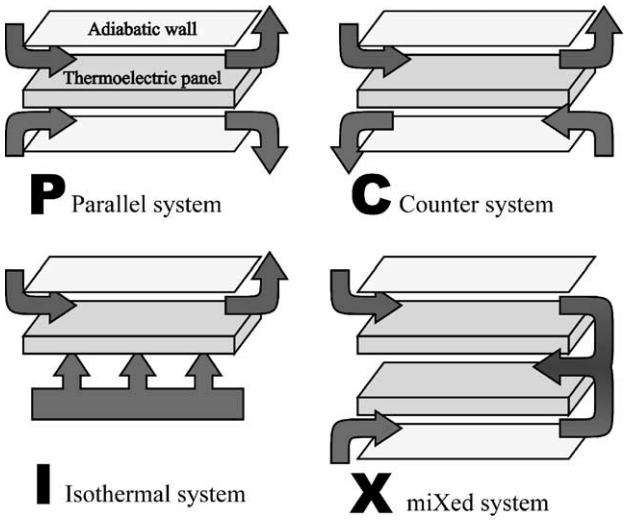

Fig. 2. Classification by the direction of fluid flow.

at the counter flow type. These two types are often selected for heat exchangers using fluids [1].

The isothermal type is the extreme case that whole a surface of the most outside of the system can be kept at a constant temperature by the infinitively large heat bath. This models, for example, the heat utilization of hot furnace wall, of phase transformation such as boiling [6], or of huge amount of seawater as the coolant. Here we discuss the case that the cold surface is kept isothermally, as shown in Fig. 2.

The mixed type uses the recycled fluids at the second stage, after the hot and cold fluid is cooled and heated, respectively, at the first heat exchange. The increment of output power is expected by getting compulsorily double amount of fluid and a medium temperature between those of hot and cold fluids.

2.3. Path shape

Secondly the path shapes of fluids are classified into three types, depending on setting of the boundary conditions: meandering type (M), helical type (H) and branched type (B), as shown in Fig. 3.

The meandering type bends the hot fluid paths, recovers the exhaust heat from the panel to which the fluid gave the heat, and will pass the heat to the next panel. This type aims at the heat recycling and the miniaturization of the system. Here we assume only one path for the cold fluid.

The helical type aims at the homogeneous ΔT for all the panels, by flowing the two fluids in counter flow. The path connection is illustrated as broken lines in Fig. 3, however, the seamless three-dimensional connection can be realized in the roll pancake model as shown in Fig. 4(a), and in the double helical model as shown in Fig. 4(b). Their detailed analysis in the cylindrical coordinate will be reported separately.

The branched type is the system that the two fluids separate equally into a few paths so that the two fluids flow side

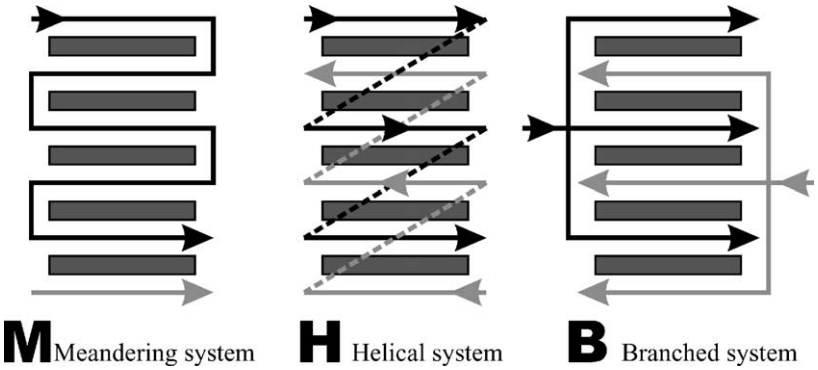

Fig. 3. Classification by the shape of fluid path.

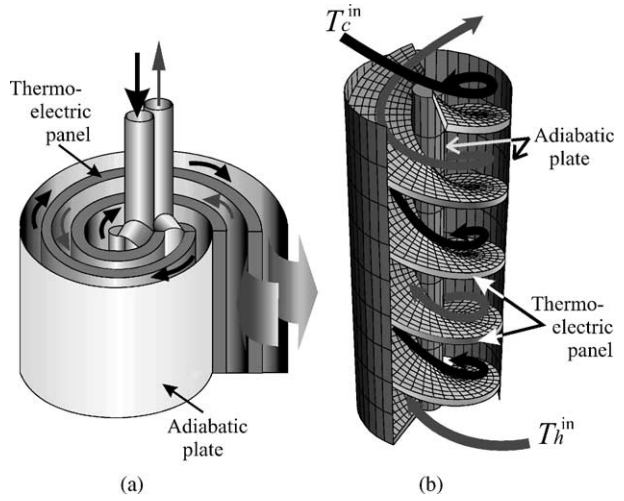

Fig. 4. Example of three-dimensional helical system: (a) roll pancake model; (b) double helical model.

by side. The number of cold paths is taken larger than that of hot paths, in case of H and B systems, because the number of paths becomes odd when the number of panels is even.

Based on the above classifications, the systems are named after the number of panel sheets (n), the direction of fluid flow (P, C, I or X) and the path shape (M, H, B). Table 1 lists the names of systems analyzed here. Under this classification, the previous conceptual proposal [4] corresponds to the mixture of 3CM and 2X.

3. Physical properties and conditions

The thermophysical properties of the thermoelectric elements in the literature scattered due to the impurities and the difference in preparation [2]. Table 2 shows a typical set of properties for an identical sample [7–10] for this work. Tables 3 and 4 show the fluid properties [11] and the parameters for thermoelectric panels. The parameters are approximated as the values at the average temperature of T_h and T_c.

The BiTe semiconductor is now available in the market. However, the large-scale power generation needs a large amount of materials. Although the thermoelectric properties of iron-base alloys are not suitable still now, they are attractive because of the natural abundance and the good electrical conductivity [12].

The liquid is superior to the gaseous fluid as the thermal carrier because of larger heat capacity, however, the gas has the advantage in corrosion of the panels and it can be often used as the exhaust gases from the industries. This study assumes the usage of inert N_2 gas as heat carrier.

In general, heat transfer coefficient, h depends mainly on the hydrodynamic behavior of the fluid and the shape of the

Table 1
Classification and abbreviation of studied system

	Shape of fluid path	Direction of fluid flow			
		Parallel (P)	Counter (C)	Mixed (X)	Isothermal (I)
One panel	–	1P	1C	–	1I
	Meandering (M)	2PM	2CM	–	2IM
			3CM		
			4CM		
Multi-panel	Helical (H)	–	2CH	–	–
			3CH		
			4CH		
	Branched (B)	–	3CB	–	–
			4CB		
Others	–	–	–	2X	2I

Table 2
Specific values of thermoelectric elements used here

Materials	Seebeck coeficient, α (μV/K)	Resistivity, ρ (μΩ m)	Thermal conductivity, λ (W/K m)	Figure of merit, Z (1/K)
Fe 23 at.% Al 20 at.% Si (p)	40.35	1.923	12.44	4.483×10^{-5}
Fe 22 at% Al (n)	−21.56	1.176	16.13	
Bi 54.3 at.% Te (p)	162	5.5	2.06	2.605×10^{-3}
Bi 64.5 at.% Te (n)	−240	10	2.02	

Table 3
Parameters for thermoelectric power generation system

Variables	Values used in this work
Thermoelectric device	
Width, w	1 m
Length, l	Variable
Thickness, d	0.05 m
Thermal sources	
Hot source	N_2 gas (inlet $T_h^{in} = 500$ K)
Cold source	N_2 gas (inlet $T_c^{in} = 300$ K)
Gas properties	
Specific heat, C_p	1044 J/kg K (at 400 K, 0.1 Pa)
Mass flow rate, M	1.00 kg/s
Heat transfer coefficient, h	500 W/m^2 K

tube surface. It was evaluated as 28.3 W/m^2 K, assuming that the turbulent flow, which obeys with Kays equation [13], flows under the hydrodynamic conditions listed in Table 4. The fins on the surfaces can improve the heat transfer coefficient, h, to a few to ten times larger values [14]. This study sets h as 500 W/m^2 K.

4. Equations for output power

4.1. Deduction of equations

Considering the system consisted of n sheets of panels as shown in Fig. 5, a set of $n + 1$ simultaneous derivative

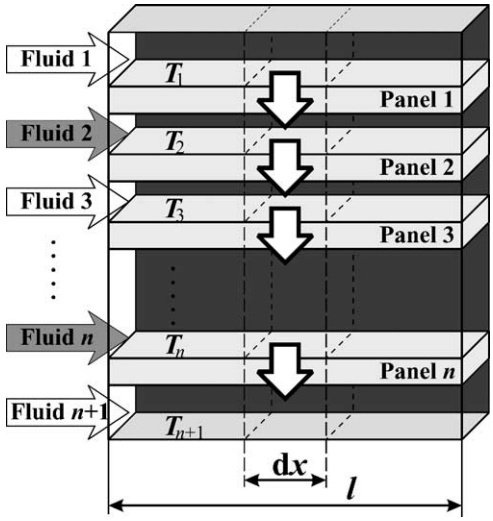

Fig. 5. Module with n panels. Direction of heat flow among fluids is illustrated.

equations can be written from the heat transfers through panels:

$$M_1 C_{p,1} \frac{dT_1(x)}{dx} = \mp K_1 w (T_1(x) - T_2(x)) \quad (1)$$

$$M_i C_{p,i} \frac{dT_i(x)}{dx} = \pm K_{i-1} w (T_{i-1}(x) - T_i(x)) \mp K_i w (T_i(x) - T_{i+1}(x)) \quad (1 < i < n) \quad (2)$$

Table 4
Hydrodynamic and boundary conditions

System	Hydrodynamic conditions	Boundary conditions
1P	$M_1 > 0$, $M_2 > 0$	$T_1(0) = T_h^{in}$, $T_2(0) = T_c^{in}$
1C	$M_1 > 0$, $M_2 < 0$	$T_1(0) = T_h^{in}$, $T_2(l) = T_c^{in}$
1I	$M_1 > 0$	$T_1(0) = T_h^{in}$, $T_2(x) = T_c^{in}$ for all x
2PM	$M_1 > 0$, $M_2 = -M_1$, $M_3 < 0$	$T_1(0) = T_h^{in}$, $T_1(l) = T_2(l)$, $T_3(l) = T_c^{in}$
2CM	$M_1 > 0$, $M_2 = -M_1$, $M_3 > 0$	$T_1(0) = T_h^{in}$, $T_1(l) = T_2(l)$, $T_3(0) = T_c^{in}$
2CH	$M_1 > 0$, $M_2 < 0$, $M_3 = M_1$	$T_1(0) = T_c^{in}$, $T_1(l) = T_3(0)$, $T_2(l) = T_h^{in}$
2IM	$M_1 > 0$, $M_2 = -M_1$	$T_1(0) = T_h^{in}$, $T_1(l) = T_2(l)$, $T_3(x) = T_c^{in}$ for all x
2I	$M_1 > 0$, $M_2 = -M_1$	$T_1(0) = T_c^{in}$, $T_2(l) = T_h^{in}$, $T_3(x) = T_c^{in}$ for all x
2X	$M_1 > 0$, $M_2 = -(M_1 + M_3)$, $M_3 > 0$	$T_1(0) = T_h^{in}$, $T_2(l) = (M_1 T_1(l) + M_3 T_3(l))/(M_1 + M_3)$, $T_3(0) = T_c^{in}$
3CM	$M_1 > 0$, $M_2 = -M_1$, $M_3 = M_1$, $M_4 > 0$	$T_1(0) = T_h^{in}$, $T_1(l) = T_2(l)$, $T_2(0) = T_3(0)$, $T_4(l) = T_c^{in}$
3CH	$M_1 > 0$, $M_2 = M_4$, $M_3 = M_1$, $M_4 < 0$	$T_1(0) = T_h^{in}$, $T_1(l) = T_3(0)$, $T_2(l) = T_4(0)$, $T_4(l) = T_c^{in}$
3CB	$M_1 > 0$, $M_2 = M_4$, $M_3 = M_1$, $M_4 < 0$	$T_1(0) = T_h^{in}$, $T_2(l) = T_c^{in}$, $T_3(0) = T_h^{in}$, $T_4(l) = T_c^{in}$
4CM	$M_1 > 0$, $M_2 = -M_1$, $M_3 = M_1$, $M_4 = -M_1$, $M_5 > 0$	$T_1(0) = T_h^{in}$, $T_1(l) = T_2(l)$, $T_2(0) = T_3(0)$, $T_3(l) = T_4(l)$, $T_5(0) = T_c^{in}$
4CH	$M_1 > 0$, $M_2 = M_4$, $M_3 = M_1$, $M_4 < 0$, $M_5 = M_1$	$T_1(0) = T_h^{in}$, $T_1(l) = T_3(0)$, $T_2(l) = T_4(0)$, $T_3(l) = T_5(0)$, $T_4(l) = T_c^{in}$
4CB	$M_1 > 0$, $M_2 = M_4$, $M_3 = M_1$, $M_4 < 0$, $M_5 = M_1$	$T_1(0) = T_c^{in}$, $T_1(l) = T_h^{in}$, $T_2(0) = T_c^{in}$, $T_3(l) = T_h^{in}$, $T_4(0) = T_c^{in}$

$$M_{n+1}C_{\mathrm{p},n+1}\frac{\mathrm{d}T_{n+1}(x)}{\mathrm{d}x} = \pm K_n w(T_n(x) - T_{n+1}(x)) \quad (3)$$

where M_i, $C_{\mathrm{p},i}$, T_i are mass flow rate, heat capacity and temperature for fluid i, w the width of the panel. The homogeneous temperature profile along y axis is assumed inside the turbulent flow. The choice of $\pm$ depends on the path condition, K_i the over-all heat transfer coefficient through the panel i,

$$K_i = \frac{1}{(1/h_{\mathrm{h},i}) + (d/\lambda) + (1/h_{\mathrm{c},i})} \quad (4)$$

$h_{\mathrm{h},i}$ and $h_{\mathrm{c},i}$ are the heat transfer coefficients between hot fluid and the panel and between cold fluid and the panel, respectively, d and λ the thickness of the panel and the average heat conductivity in the panel, respectively.

$$\lambda = \frac{\lambda_{\mathrm{p}}s_{\mathrm{p}} + \lambda_{\mathrm{n}}s_{\mathrm{n}}}{s_{\mathrm{p}} + s_{\mathrm{n}}} \quad (5)$$

where λ_{p} and λ_{n} are heat conductivity of p and n type elements, respectively, s_{p} and s_{n} the cross-sectional area of these elements. For simplicity, heat transfer by Peltier effect and exothermal heat by Joule effect are neglected. The detailed considerations on this simplicity will be reported separately.

By replacing:

$$A_{i,j} = \frac{K_i w}{M_j C_{p,j}}, \quad (6)$$

the simultaneous equations can be written in the matrix form as,

$$\frac{\mathrm{d}}{\mathrm{d}x}\begin{bmatrix} T_1(x) \\ T_2(x) \\ \vdots \\ T_n(x) \\ T_{n+1}(x) \end{bmatrix} = \begin{bmatrix} \mp A_{11} & \pm A_{11} & & & 0 \\ \pm A_{12} & \mp(A_{12}+A_{22}) & \pm A_{22} & & \\ & \ddots & \ddots & \ddots & \\ & & \pm A_{n-1,n} & \mp(A_{n-1,n}+A_{n,n}) & \pm A_{n,n} \\ 0 & & & \pm A_{n,n+1} & \mp A_{n,n+1} \end{bmatrix} \begin{bmatrix} T_1(x) \\ T_2(x) \\ \vdots \\ T_n(x) \\ T_{n+1}(x) \end{bmatrix} \quad (7)$$

The equation is solved for x by setting the boundary conditions, as listed in Table 4. The mathematical software, Mathematica, was partially used as a tool [15]. The solutions, $T_i(x)$, are described later. The temperature $\theta_{i,j}(x)$ at the surface of the panel i facing to the fluid j is written using $T_i(x)$.

$$\theta_{i,i}(x) = T_i(x) - \frac{K_i}{h_i}(T_i(x) - T_{i+1}(x)) \quad (8)$$

$$\theta_{i,i+1}(x) = T_{i+1}(x) + \frac{K_i}{h_{i+1}}(T_i(x) - T_{i+1}(x)) \quad (9)$$

The electromotive force, E, is the summation of the temperature difference over all the panels.

$$E = \sum_{i=1}^{n}\left|\sum_{\mathrm{panel}}\alpha(\theta_{i,i} - \theta_{i,i+1})\right| \quad (10)$$

$$E = \sum_{i=1}^{n}\left|n_x n_y \int_0^w\int_0^l \alpha(\theta_{i,i}(x) - \theta_{i,i+1}(x))\,\mathrm{d}x\,\mathrm{d}y\right| \quad (11)$$

where α is the difference between those of p and n elements, n_x and n_y the number densities of thermoelectric pairs in the direction x and y, respectively. Note that $n_x n_y = 1/(s_{\mathrm{p}}+s_{\mathrm{n}})$. The electric resistance, R_i is given as:

$$R_i = n_x n_y\, wld\left(\frac{\rho_{\mathrm{p}}}{s_{\mathrm{p}}} + \frac{\rho_{\mathrm{n}}}{s_{\mathrm{n}}}\right) \quad (12)$$

where ρ_{p} and ρ_{n} are the specific resistivity of p and n elements. The maximum output power, P optimized by balancing the internal and external resistance as used in normal way:

$$P = \frac{E^2}{4\sum_{i=1}^{n}R_i} \quad (13)$$

This work uses hereafter this P, where the internal and external resistance are the same.

4.2. Output power of 1P system

The simultaneous equations are solved at the 1P system, where one sheet of panel is exposed in parallel flow.

$$T_{\mathrm{h}}(x) = \frac{M_{\mathrm{h}}C_{\mathrm{p,h}}T_{\mathrm{h}}^{\mathrm{in}} + M_{\mathrm{c}}C_{\mathrm{p,c}}((T_{\mathrm{h}}^{\mathrm{in}} - T_{\mathrm{c}}^{\mathrm{in}}) \times\exp(-DKwx) + T_{\mathrm{c}}^{\mathrm{in}})}{M_{\mathrm{h}}C_{\mathrm{p,h}} + M_{\mathrm{c}}C_{\mathrm{p,c}}} \quad (14)$$

$$T_{\mathrm{c}}(x) = \frac{M_{\mathrm{h}}C_{\mathrm{p,h}}(T_{\mathrm{h}}^{\mathrm{in}} - (T_{\mathrm{h}}^{\mathrm{in}} - T_{\mathrm{c}}^{\mathrm{in}})\exp(-DKwx)) + M_{\mathrm{c}}C_{\mathrm{p,c}}T_{\mathrm{c}}^{\mathrm{in}}}{M_{\mathrm{h}}C_{\mathrm{p,h}} + M_{\mathrm{c}}C_{\mathrm{p,c}}} \quad (15)$$

where

$$D = \frac{1}{M_{\mathrm{h}}C_{\mathrm{p,h}}} + \frac{1}{M_{\mathrm{c}}C_{\mathrm{p,c}}} \quad (16)$$

The electromotive force is calculated by integrating the above results in Eq. (11),

$$E = \frac{M_{\mathrm{h}}M_{\mathrm{c}}C_{\mathrm{p,h}}C_{\mathrm{p,c}}n_x n_y\,\mathrm{d}\alpha(T_{\mathrm{h}}^{\mathrm{in}} - T_{\mathrm{c}}^{\mathrm{in}})(1 - \exp(-DKwl))}{(M_{\mathrm{h}}C_{\mathrm{p,h}} + M_{\mathrm{c}}C_{\mathrm{p,c}})\lambda} \quad (17)$$

The output power P_1 is obtained using Eq. (13).

$$P_1 = \frac{M_{\mathrm{h}}^2M_{\mathrm{c}}^2C_{\mathrm{p,h}}^2C_{\mathrm{p,c}}^2n_x n_y\,\mathrm{d}\alpha^2(T_{\mathrm{h}}^{\mathrm{in}} - T_{\mathrm{c}}^{\mathrm{in}})^2 \times\{1 - \exp(-DKwl)\}^2}{4wl(M_{\mathrm{h}}C_{\mathrm{p,h}} + M_{\mathrm{c}}C_{\mathrm{p,c}})^2(\rho_{\mathrm{p}}/s_{\mathrm{p}} + \rho_{\mathrm{n}}/s_{\mathrm{n}})\lambda^2} \quad (18)$$

P_1 agreed with the solution reduced by Laplace transformation [3], when our assumptions were introduced. The

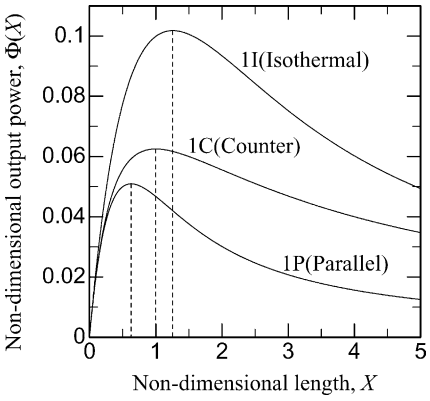

Fig. 6. Non-dimensional output of one-panel systems.

temperature difference, $\theta_h(x) - \theta_c(x)$, agreed with the previous analysis of parallel flow [5].

Especially when all the terms of $M_i C_{p,i}$ are equivalent and all K_i are equal to a constant K, we obtain the output power P_2 in a simple form,

$$P_2 = MC_p \frac{Kd}{\lambda} Z(T_h^{in} - T_c^{in})^2 L(s_p, s_n) \Phi_{1P}(X) \tag{19}$$

where Z is the figure of merit, known as the material parameter [2,10], and $\Phi_{1P}(X)$ the new non-dimensional function.

$$Z = \frac{(\alpha_p - \alpha_n)^2}{(\sqrt{\rho_p \lambda_p} + \sqrt{\rho_n \lambda_n})^2} \tag{20}$$

$$L(s_p, s_n) = \frac{s_p s_n (\sqrt{\rho_p \lambda_p} + \sqrt{\rho_n \lambda_n})^2}{(\lambda_p s_p + \lambda_n s_n)(\rho_p s_n + \rho_n s_p)} \tag{21}$$

$$\Phi_{1P}(X) = \frac{(1 - e^{-2X})^2}{16X} \tag{22}$$

where the non-dimensional length of the system X is defined as,

$$X = \frac{Kwl}{MC_p} \tag{23}$$

$\Phi_{1P}(X)$ is characteristic for each system as shown in Fig. 6 and Table 5. $L(s_p, s_n)$ the function of the cross-sectional area, and its maximum is 1 when:

$$\frac{s_n}{s_p} = \sqrt{\frac{\rho_n \lambda_p}{\rho_p \lambda_n}} \tag{24}$$

The maximum $\Phi_{1P}(X) = 5.091 \times 10^{-2}$ when:

$$4X + 1 = e^{2X} \tag{25}$$

This Eq. (25) can be numerically solved as $X = 0.6282$. P_3 is obtained after these maximizations of $L(s_p, s_n)$ and $\Phi_{1P}(X)$ for Eq. (19).

$$P_3 = \Phi_{1P}(X)_{max} MC_p \frac{Kd}{\lambda} Z(T_h^{in} - T_c^{in})^2 \tag{26}$$

P_3 depends on the mass flow through M, h_h and h_c, as well as the figure of merit and the square of temperature difference. $\Phi_{1P}(X)$max is constant independent of the materials and fluid properties, and it is also the parameter determined by the system design. Therefore, we define $\gamma(1P) = \Phi_{1P}(X)$max as the system parameter, and $\delta(1P) = 0.6282$ as the characteristic length, specialized for 1P system. These are listed in Table 6.

The contributions of s_p and s_n through the terms of K and λ were neglected because they were small.

4.3. Output power of 1C and 1I system

The simultaneous Eq. (7) are solved at the 1C system, and the thermoelectric force E and the output power P_1 are calculated in the same procedure as described above.

$$E = \frac{M_h M_c C_{p,h} C_{p,c} n_x n_y \, d\alpha (T_h^{in} - T_c^{in})(1 - \exp(-DKwl))}{(M_h C_{p,h} \exp(-DKwl) + M_c C_{p,c})\lambda} \tag{27}$$

$$P_1 = \frac{M_h^2 M_c^2 C_{p,h}^2 C_{p,c}^2 n_x n_y \, d\alpha^2 (T_h^{in} - T_c^{in})^2 \times \{1 - \exp(-DKwl)\}^2}{4wl\{M_h C_{p,h} \exp(-DKwl) + M_c C_{p,c}\}^2 \times (\rho_p/s_p + \rho_n/s_n)\lambda^2} \tag{28}$$

When $M_h C_{p,h} = |M_c C_{p,c}|$,

$$P_2 = MC_p \frac{Kd}{\lambda} Z(T_h^{in} - T_c^{in})^2 L(s_p, s_n) \Phi_{1C}(X) \tag{29}$$

where $L(s_p, s_n)$ is identical with Eq. (21). The function of $\Phi_{1C}(X)$ is given in Table 5, and the characteristic parameters, $\delta(1C) = 1$ and $\Phi_{1C}(X)$max $= \gamma(1C) = 1/16$, are listed in Table 6.

Similarly P_1 for 1I system is given by:

$$P_1 = \frac{M_h^2 C_{p,h}^2 n_x n_y \, d\alpha^2 (T_h^{in} - T_c^{in})^2}{4wl(\rho_p/s_p + \rho_n/s_n)\lambda^2} \times \left\{1 - \exp\left(-\frac{Kwl}{M_h C_{p,h}}\right)\right\}^2 \tag{30}$$

It is mathematically proved that P_1 for 1I system is a limit of those for 1P and 1C systems, as M_c approaches infinity. P_2 for 1I system is also written in the similar equation with Eq. (29). $\Phi_{1I}(X)$, $\delta(1I)$ and $\gamma(1C)$ are shown in Tables 5 and 6. As M_h approaches infinity in Eq. (30), the system corresponds to the case where the both surfaces are heated and cooled by the infinitively large heat baths. We obtain the well-known output,

$$P = \frac{n_x n_y w l \alpha^2 (T_h - T_c)^2}{4d(\rho_p/s_p + \rho_n/s_n)} \tag{31}$$

where P becomes the maximum at $s_n/s_p = (\rho_n/\rho_p)^{1/2}$.

In a short summary, the non-dimensional output Φ depends on the fluid direction, but the formula can be commonly written only by the same length parameter X. Three $\Phi(x)$ for one sheet of panel are compared in Fig. 6.

Table 5
Calculated non-dimensional output power $\Phi(X)$

System	$\Phi(X)$
1P	$\Phi(X) = \dfrac{(1-\mathrm{e}^{-2X})^2}{16X}s$
1C	$\Phi(X) = \dfrac{X}{4(1+X)^2}$
1I	$\Phi(X) = \dfrac{(1-\mathrm{e}^{-X})^2}{4X}$
2PM	$\Phi(X) = \dfrac{\{-1+\sqrt{2}-(1+\sqrt{2})\mathrm{e}^{2\sqrt{2}X}+2\mathrm{e}^{(1+\sqrt{2})X}\}^2}{2\{2-\sqrt{2}+(2+\sqrt{2})\mathrm{e}^{2\sqrt{2}X}\}^2X}$
2CM	$\Phi(X) = \dfrac{(1-\mathrm{e}^{-X})^2}{8X}$
2CH	$\Phi(X) = \dfrac{1}{2X(2+\coth X)^2}$
2IM	$\Phi(X) = \dfrac{\{-\sqrt{5}\mathrm{e}^{X/2}+\sqrt{5}\cosh(\sqrt{5}X/2)+3\sinh(\sqrt{5}X/2)\}^2}{8X\{2+3\cosh(\sqrt{5}X)+\sqrt{5}\sinh(\sqrt{5}X)\}}$
2I	$\Phi(X) = \dfrac{\mathrm{e}^{(-1-\sqrt{5})X}\{(-3+\sqrt{5})\mathrm{e}^{X/2}-2\sqrt{5}\mathrm{e}^{\sqrt{5}X/2}+(3+\sqrt{5})\mathrm{e}^{(1/2+\sqrt{5})X}\}^2}{32X\{-2+7\cosh(\sqrt{5}X)+3\sqrt{5}\sinh(\sqrt{5}X)\}}$
2X	$\Phi(X) = \dfrac{(1-\mathrm{e}^{-X})^2}{8X}$
3CM	$\Phi(X) = \dfrac{\{-1+(1+2X)\cosh(\sqrt{2}X)\}^2}{6X\{\sqrt{2}(2+X)\cosh(\sqrt{2}X)+\sinh(\sqrt{2}X)\}^2}$
3CH	$\Phi(X) = \dfrac{\{2X\cosh(X/\sqrt{2})+\sqrt{2}\sinh(X/\sqrt{2})\}^2}{3X\{(2+4X)\cosh(X/\sqrt{2})+\sqrt{2}(2+X)\sinh(X/\sqrt{2})\}^2}$
3CB	$\Phi(X) = \dfrac{[\sqrt{2}\{-1+(1+4X)\cosh(2\sqrt{2}X)\}+(1+6X)\sinh(2\sqrt{2}X)]^2}{12X[\sqrt{2}\{-1+(3+4X)\cosh(2\sqrt{2}X)\}+2(2+3X)\sinh(2\sqrt{2}X)]^2}$
4CM	$\Phi(X) = \dfrac{1}{4X}\dfrac{\begin{array}{l}[-2\mathrm{e}^{(1+3\sqrt{5})X/2}(-1+\mathrm{e}^X)(11+3\mathrm{e}^X)+e^X\{-11-5\sqrt{5}+(7-3\sqrt{5})\mathrm{e}^X\}+\mathrm{e}^{(1+3\sqrt{5})X}\{-11-5\sqrt{5}+(7+3\sqrt{5})\mathrm{e}^X\} \\ +\mathrm{e}^{\sqrt{5}X}[10-6\sqrt{5}+\mathrm{e}^X\{-11+3\sqrt{5}+(-3+\sqrt{5})\mathrm{e}^X\}]+\mathrm{e}^{2\sqrt{5}X}[-10-6\sqrt{5}+\mathrm{e}^X\{11+3\sqrt{5}+(3+\sqrt{5})\mathrm{e}^X\}] \\ +\mathrm{e}^{(1+\sqrt{5})X/2}[-1-\sqrt{5}+\mathrm{e}^X\{8-6\sqrt{5}-(7-3\sqrt{5})\mathrm{e}^X\}]+\mathrm{e}^{(1+5\sqrt{5})X/2}[-1+\sqrt{5}+\mathrm{e}^X\{8+6\sqrt{5}-(7+3\sqrt{5})\mathrm{e}^X\}]]^2\end{array}}{\{(5-3\sqrt{5})\mathrm{e}^X+10\mathrm{e}^{\sqrt{5}X}+(5+3\sqrt{5})\mathrm{e}^{(1+2\sqrt{5})X}\}^2\{(-3+\mathrm{e}^X)(-1+\mathrm{e}^{\sqrt{5}X})+\sqrt{5}(-1+\mathrm{e}^X)(1+\mathrm{e}^{\sqrt{5}X})\}^2}$
4CH	$\Phi(X) = \dfrac{1}{4X}\dfrac{\begin{array}{l}\{l5\mathrm{e}^{2\sqrt{5}X}-5\sqrt{5}\mathrm{e}^{(1+\sqrt{5})X}-5\mathrm{e}^{2(1+\sqrt{5})X}+5\sqrt{5}\mathrm{e}^{(1+3\sqrt{5})X}-2(5+\sqrt{5})\mathrm{e}^{3(1+\sqrt{5})X/2}-2(-5+\sqrt{5})\mathrm{e}^{(1+3\sqrt{5})X/2} \\ +2(5+\sqrt{5})\mathrm{e}^{(1+5\sqrt{5})X/2}+2(-5+\sqrt{5})\mathrm{e}^{(3+5\sqrt{5})X/2}\}^2\end{array}}{\begin{array}{l}\{15\mathrm{e}^{\sqrt{5}X}-8e^{(1+\sqrt{5})X}-5\mathrm{e}^{(2+\sqrt{5})X}-20\mathrm{e}^{3(1+\sqrt{5})X/2}-20\mathrm{e}^{(3+\sqrt{5})X/2}+4(5-2\sqrt{5})\mathrm{e}^{(1+\sqrt{5})X/2} \\ +(9-10\sqrt{5})\mathrm{e}^X+4(5+2\sqrt{5})\mathrm{e}^{(1+3\sqrt{5})X/2}+(9+10\sqrt{5})\mathrm{e}^{(1+2\sqrt{5})X}\}^2\end{array}}$
4CB	$\Phi(X) = \dfrac{\{-1+\mathrm{e}^{5X}(1+45X)\}^2}{4X\{2-9\mathrm{e}^{5X}(3+10X)\}^2}$

The outputs are calculated using the materials parameters in Table 2 for the BiTe semiconductors and for the FeAl alloys. As shown in Fig. 7, the maximum power for BiTe semiconductor requires a characteristic panel length 3.76 times longer than that of FeAl alloys, but it gains 106 times larger output power, when the panel thickness d is the same. Because the ratio of Z in both materials is 58.1, the worse heat conductance of BiTe causes the larger difference in output power. For the materials selection for thermoelectric panels, therefore, the total output power and the prices of materials and fluid will be considered entirely, as we pointed previously [12]. In case of thinner BiTe panel ($d = 0.005$ m), for example, the output power decreased although the panel length can be shortened. This shows that the optimal thickness of the panel exists depending on a certain length, as re-

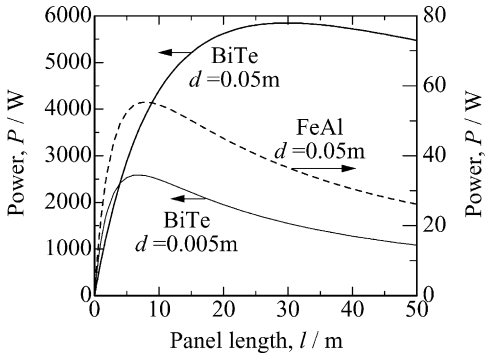

Fig. 7. Output power of 1C system, where N_2 gases of 1 kg/s at 500 and 300 K are flown over a panel of 1 m width with counter flow, d is the panel thickness.

Table 6
Analyzed non-dimensional parameters

System	System parameter, γ	Characteristic length, δ	Output per unit length, $\gamma/\delta/n$
1P	0.050908	0.62822	0.08104
1C	1/16 = 0.0625	1	0.06250
1I	0.101816	1.25643	0.08104
2PM	0.050881	1.77891	0.01430
2CM	0.050908	1.25643	0.02026
2CH	0.058289	0.41581	0.07009
2X	0.050908	1.25643	0.02026
2I	0.091863	0.63631	0.07218
2IM	0.092222	1.69764	0.02716
3CM	0.045203	1.73604	0.00858
3CH	0.059231	0.28820	0.06851
3CB	0.056444	0.30489	0.06171
4CM	0.040966	2.07989	0.00492
4CH	0.060183	0.22504	0.06686
4CB	0.059793	0.24565	0.06085

ported experimentally [16]. Fig. 8 shows the optimal thickness evaluated from Eq. (29). Our deduced equations are thus the base for system design of thermoelectric power generation.

4.4. Output power of n sheets of panels

The equations are calculated in the system having n sheets of panels. The analytical solutions, P_1, are obtained in the same sequence of Section 4.1 and under the conditions listed in Table 4. The obtained equations are complex and very long expression. When they are simplified by setting all K_i identical and $M_h C_{p,h} = |M_c C_{p,c}|$, the output power, P_2, in all the systems can be commonly described as Eq. (19) or (29) by the non-dimensional output $\Phi(X)$. They are listed in Table 5, where the comparison among the systems becomes possible, independently of thermoelectric materials and of the thermophysical properties of fluids.

Figs. 9 and 10 show X dependency of $\Phi(X)$. Only one maximum commonly exists for each $\Phi(X)$. The system parameter γ and the characteristic length δ are evaluated numerically in Table 6.

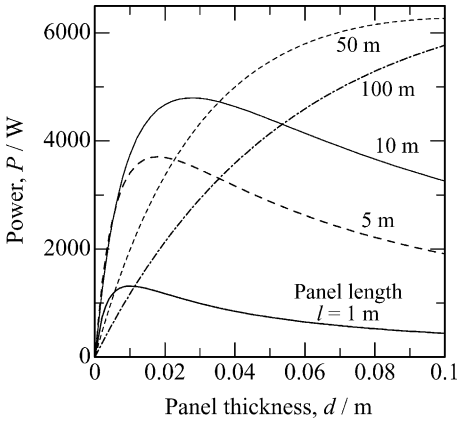

Fig. 8. Output power of 1C system, where N_2 gases of 1 kg/s at 500 and 300 K are flown over a BiTe panel of 1 m width with counter flow.

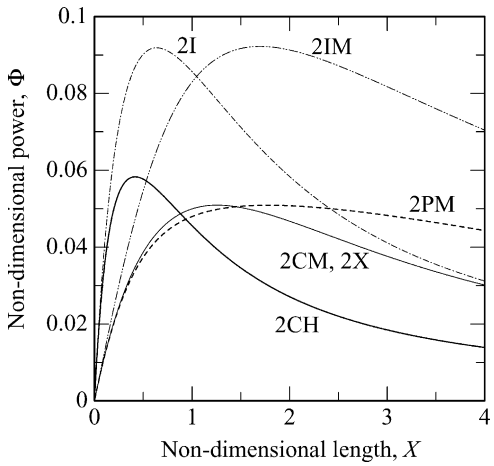

Fig. 9. Non-dimensional output of the two-panel systems.

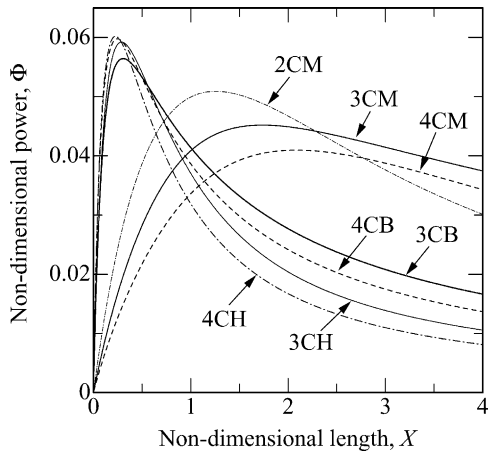

Fig. 10. Non-dimensional output of the three- and four-panel systems.

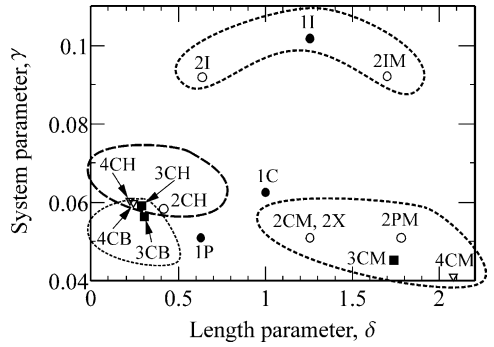

Fig. 11. Comparison of thermoelectric power generation systems.

5. Discussions

The system parameter, γ are summarized in Fig. 11.

Firstly, γ(1I), γ(2I) and γ(2IM) are significantly high, because a cold surface is kept at a constant temperature for

these systems. It was basically assumed in the isothermal type (I) that the infinitive fast heat supply and heat compensation was available to keep a constant temperature. This assumption was mathematically realized that a limit of 1P and 1C system was 1I system as M approached to the infinitive. The infinitive fast cooling in I type is the reason of high power.

Secondly, the power of 1C is larger than that of 1P, while the characteristic length of 1C is longer. As shown in Fig. 6, Φ(1C) is larger than Φ(1P) for all X. The tendency that the counter flow can generate larger power than the parallel flow is valid also in two sheets of panels: γ(2CM) > γ(2PM). However, the output per unit length of panel is the highest for 1P and 1I, as listed in Table 6. The efficiency in thermoelectric panel is better for 1P and 1I than for 1C, although the efficiency of heat is the best for 1C.

When we compare by the path shapes (H, B and M), the helical type has the highest γ and the shortest length δ. The branched type is a little smaller γ and a little longer δ than those of H type. The geometrical construction of H type seems possible as shown in Fig. 4, although the total path length for fluid becomes longer, which causes larger pressure loss. Considering the pumping power of fluid [5], therefore, the latter may have still the potential for application.

As the number of sheets of panels increases for H and B types, their system parameters γ increase and their characteristic lengths δ become shorter. In H and B types, the multi-panel construction thus improves the thermoelectric properties, however, it decreases them for M types. Meandering type needs the longest δ in these three types. Namely, heat recycling by M type needs plenty of thermo-elements. If we can use the cheaper thermoelements in future, the exhaust heat from the thermoelectric generators will be recovered.

Except for isothermal types, the highest output parameter γ is obtained in 1C system. γ becomes gradually smaller at 4CH, 4CB, 3CH, 2CH, 3CB systems in this order. γ(multi-panels systems) gets closer to γ(1C), as the number of sheets increases in H and B types.

The shortest length is achieved at 4CH system, where the difference with output of 1C system is only 3.71% and the length of 4CH is 77.5% shorter. Therefore, the output per unit length of panel is higher for H types than 1C.

In summary, the multiplication of panels decreases the output a little, but it can shorten the length of thermoelectric power generator.

6. Conclusion

This work deduced analytically the output P_1 for 15 systems of flat thermoelectric panels, based on heat transfer theory. Setting the heat permeability K, mass flow rate M and specific heat of fluids C_p identical, the output P_2 can be written by non-dimensional functions $\Phi(X)$. The maximum output P_3 is determined as:

$$P_3 = \gamma M C_p \frac{Kd}{\lambda} Z (T_h^{in} - T_c^{in})^2 \quad (32)$$

The system parameter γ is characteristic for geometry of path and the direction of fluid. γ were significantly large for isothermal systems. In the other systems, γ was largest for the system of the counter flow with one panel (1C). The multiplication of thermoelectric panels can shorten significantly the system length, i.e. the device area, although the outputs from the multi-panels decrease a few percent.

The effect of thermoelectric material properties on the output in thermoelectric power generation has been considered representative only by the figure of merit, Z. However, as written in Eq. (32), λ has the contribution to the output stronger than as expected previously, when the fluids are working. Under the fixed conditions given by such as M, C_p, Z and ΔT, the output is a function of the term K/λ in Eq. (32). The better heat transfer to/from the surface and the worse heat conductivity of the panel are desired.

Acknowledgements

The authors thank to Prof. Emeritus of Kyoto University, Katsutoshi Ono and Mr. Masashi Kihara for their advices and discussions. This work was financially supported in part by Yazaki foundation, Japan Nuclear Cycle Development Institute and Sekisui Chemical Co. Ltd.

References

[1] S. Isshiki, N. Kitayama, Technology of Heat Transfer, Morikita Press, Tokyo, 1984.
[2] R. Sakata (Ed.), Thermoelectrics, Principles and Applications, Realize Inc., Tokyo, 2001.
[3] B. Mathiprakasam, T. Sutikno, J. Beeson, in: Proceedings of the Fourth International Conference on Thermoelectrics, IEEE, Piscataway, NJ, 1982, p. 61.
[4] K. Ono, R.O. Suzuki, Proceedings of the 17th International Conference on Thermoelectrics, IEEE, Piscataway, NJ, 1998, pp. 515–518.
[5] J. Esarte, G. Min, D.M. Rowe, J. Power Sources 93 (2001) 72–76.
[6] T. Kyono, R.O. Suzuki, K. Ono, IEEE Transition on Energy Conversion, 2003, in press.
[7] K. Ono, R.O. Suzuki, R. Nakahashi, M. Shoda, Tetsu-to-Hagané 83 (2) (1997) 157–161.
[8] M. Shoda, M. Kado, T. Tsuji, R.O. Suzuki, K. Ono, Tetsu-to-Hagané 84 (2) (1998) 154–158.
[9] K. Ono, M. Kado, R.O. Suzuki, Steel Res. 69 (9–98) (1998) 387–390.
[10] D.M. Rowe, CRC Handbook of Thermoelectrics, CRC Press, Boca Raton, 1995.
[11] Thermophysical Properties of Fluids, Jpn. Soc. Mech. Eng., Jpn. Soc., Mech. Eng., Tokyo, 1986.
[12] K. Ono, R.O. Suzuki, J. Metals 12 (1998) 49–51.
[13] W.M. Kays, M.E. Crawford, Convective Heat and Mass Transfer, 2nd ed., McGraw-Hill, NY, 1980.
[14] Heat Transfer, 4th ed., Jpn. Soc., Mech. Eng., Jpn. Soc., Mech. Eng., Tokyo, 1986.
[15] S. Wolfram, The Mathematica Book, 4th ed., Wolfram Media/Cambridge University Press, 1999.
[16] M. Sakamoto, S. Kagawa, in: Proceedings of Symposium for Thermoelectric Conversion 1999 (TEC'99), Thermoelectric Conversion Society of Japan, Fujisawa, Japan, 1999, pp. 40–41.